SMART: Robust absorbing layer and *S*-waves filtering for acoustic anisotropic wave simulation

L. Métivier, LJK-CNRS, Université Grenoble Alpes, R. Brossier, ISTerre, Université Grenoble Alpes, S. Operto Géoazur-CNRS, Université Nice Sophia Antipolis, J. Virieux, ISTerre, Université Grenoble Alpes*

SUMMARY

At the exploration scale, the simulation of seismic wave propagation in the subsurface requires using absorbing boundary conditions. For the last twenty years, the method of choice has been the Perfectly Matched Layer (PML) method. PML are easy to implement and remarkably accurate. However, in certain situations such as the simulation of seismic waves in anisotropic media, the PML method becomes amplifying. We present here an alternative layer method, the SMART method. This method is based on a selective damping strategy. From an eigenvalue analysis of the matrices defining the hyperbolic system, the outgoing components of the wavefield associated with *P*- and *S*-wave velocities are damped. The SMART layer has two advantages over the PML. First, the dissipation is ensured for elasto-dynamic equations in isotropic and anisotropic media (no amplification). Second, the method yields a new strategy to prevent from the generation of non physical *S*-waves in acoustic transverse isotropic modeling. The SMART layer method is not perfectly matched, therefore less accurate than the PML. However our numerical experiments show that the accuracy of the PML can be reached provided an increase of the layer width. The additional computational cost associated with this increase of the layer size is compensated by the fact that the SMART method is less expensive: only a zero-order term is added to the initial system of equations, no additional variables are required.

INTRODUCTION

At the seismic exploration scale, the subsurface is seen as a semi-infinite medium. Modeling the propagation of seismic wave beneath the free surface requires using appropriate boundary conditions to avoid the generation of unwanted reflections. The design of absorbing boundary conditions for wave propagation has been investigated for almost 40 years, since the pioneering work of Engquist and Majda (1977) and the design of first-order radiation boundary conditions for the wave equation. In the quest of designing accurate absorbing boundary conditions, the Perfectly Matched Layers (PML) method proposed by Bérenger (1994) has been a milestone. Similarly to the sponge layer of Cerjan et al. (1985), the domain of interest is surrounded by a layer in which the wavefield is damped. The main interesting property of the PML is that the reflection coefficient at the interface between the domain of interest and the absorbing layer is zero in the continuous formulation*, for all incidence angles. Originally introduced for the 2D Maxwell's equations, the PML strategy has been rapidly extended to the elasto-dynamic equations, and has reached the status of reference absorbing method for seismic wave propagation.

However, some cases exist in which the method faces difficulties. In particular, when applied to seismic wave simulation in anisotropic media, the PML method becomes amplifying. This phenomenon has first been exhibited by Becache et al. (2003) for the elasto-dynamic equation in orthorombic media. It has been later on reported for the simulation of wave in transversely isotropic (TI) media under the acoustic approximation (Operto et al., 2009; Duveneck and Bakker, 2011). Nevertheless, an accurate modeling of seismic wave propagation at the exploration scale requires accounting for the upper-crust anisotropy. Imaging methods such as Full Waveform Inversion (FWI) and Reverse Time Migration (RTM) require accounting for the anisotropy to yield reliable subsurface parameter estimations.

In this study, we present an alternative layer method named SMART layer. This method has been proposed by Halpern et al. (2011), as a generalization of the 1D method of Israeli and Orszag (1981). It is based on a numerical analysis of hyperbolic systems which provides a local decomposition of the wavefield into components propagating inward and outward the medium, in each direction of the Cartesian system of coordinates. Only the outgoing components are damped, depending on the position of the layer. The method amounts to add a zero-order term to the original set of partial differential equations used to describe the wave propagation.

The method presents two advantages over the PML method for the simulation of seismic waves in anisotropic media. First, the dissipation of the energy of the solution is ensured: no amplification is possible in any cases. This results because the zero-order term which is introduced is dissipative for the energy of the solution, provided that the original set of equations satisfies a symmetrizability condition. This condition is satisfied by the general elasto-dynamic equations, in isotropic and anisotropic media. Second, in acoustic TI modeling, the generation of non physical *S*-waves can be prevented. In the local decomposition of the wavefield, each component is associated with a particular wave velocity. This provides a way to damp the unwanted *S*-waves directly around the point-source.

Compared to the PML, the SMART layer is not perfectly matched, and therefore, less accurate. The reflection coefficient at the interface between the layer and the domain of interest is zero only for waves propagating at normal incidence in the continuous formulation. However, the accuracy of the method can be controlled by the size of the layer. Compared to the PML and its CPML variant (Komatitsch and Martin, 2007), the SMART layer does not require any splitting of the unknowns or additional memory variables. Therefore, for the same computational cost, the SMART method can be used with a larger layer.

The study is organized as follows. We introduce the principle of the SMART method with simple 1D and 2D examples. We provide numerical illustrations of efficiency of this method for 2D acoustic TI equations. The experiments are performed

*and almost zero after discretization

DOI http://dx.doi.org/10.1190/segam2014-0860.1

on a variable tilt angle model extracted from the BP 2007 anisotropic benchmark model. The robustness of the SMART layer is emphasized, compared to the PML. We show that the accuracy of the PML can be reached using the SMART layer at the expense of the introduction of 10 additional grid points in the layer. We finally illustrate the efficiency of the SMART method to prevent the generation of spurious *S*-waves. A conclusion is given in the last section.

THE SMART LAYER METHOD

A 1D example

Consider the first-order acoustic wave system

$$\begin{cases} \partial_t u_z = \frac{1}{\rho_0}\partial_z p \\ \partial_t p = \rho_0 c_0^2 \partial_z u_z + s_p, \end{cases} \tag{1}$$

where $u_z(z,t)$ is the vertical velocity displacement, $p(z,t)$ is the pressure wavefield, c_0 and ρ_0 are constant *P*-wave velocity and density, $s_p(z,t)$ is an explosive source term. The system (1) can be rewritten as

$$\partial_t u + A_0 \partial_z u = s, \tag{2}$$

where

$$u = [u_z \;\; p]^T, \;\; s = [0 \;\; s_p]^T, \;\; A_0 = -\begin{pmatrix} 0 & \frac{1}{\rho_0} \\ \rho_0 c_0^2 & 0 \end{pmatrix}. \tag{3}$$

The matrix A_0 is diagonalizable. Its eigenvalues are c_0 and $-c_0$. We denote P the change of coordinates matrix associated with the diagonalization and we define $v(z,t) = Pu(z,t)$ solution of

$$\begin{cases} \partial_t v_1 = c_0 \partial_z v_1 + (Ps)_1 \\ \partial_t v_2 = -c_0 \partial_z v_2 + (Ps)_2. \end{cases} \tag{4}$$

The system (4) consists in the superposition of the propagation of two plane waves: $v_1(z,t)$ propagates downward, while $v_2(z,t)$ propagates upward. Absorbing outgoing waves thus becomes easy: one only needs to introduce damping terms $d^+(z)v_1(z,t)$ and $d^-(z)v_2(z,t)$ in the first and second equation of system (4). The coefficients $d^+(z)$ and $d^-(z)$ are zero in the domain of interest and grow smoothly in absorbing layers defined at the top and the bottom of the 1D domain. Defining the matrices

$$E^+ = \begin{pmatrix} 1 & 0 \\ 0 & 0 \end{pmatrix}, \;\; E^- = \begin{pmatrix} 0 & 0 \\ 0 & 1 \end{pmatrix}, \tag{5}$$

the introduction of the absorbing layer thus amounts to modify the initial system (2) as

$$\partial_t u + A_0 \partial_z u + d(z)^+ P^T E^+ P u + d(z)^- P^T E^- P u = s. \tag{6}$$

Multi-dimensional generalization

The strategy described above has been proposed by Israeli and Orszag (1981). The generalization to a multi-dimensional case is proposed by Halpern et al. (2011). The principle is the same: the wavefield is decomposed locally into components propagating inward and outward the domain of interest. Only outgoing components are damped. The selection of the components to be damped depends on the layer position. In 2D, for instance, in the right layer, we will damp only components propagating in the positive x direction.

The key issue is the local decomposition to be performed. Coming back to the 1D case, one should note that the operators $P^T E^+ P$ and $P^T E^- P$ are actually the projectors on the eigenspaces of the matrix A_0. Consider the 2D acoustic wave propagation equations

$$\partial_t u + A_1 \partial_x u + A_2 \partial_z u = s, \tag{7}$$

where

$$A_1 = -\begin{pmatrix} 0 & 0 & \frac{1}{\rho_0} \\ 0 & 0 & 0 \\ \rho_0 c_0^2 & 0 & 0 \end{pmatrix}, \;\; A_2 = -\begin{pmatrix} 0 & 0 & 0 \\ 0 & 0 & \frac{1}{\rho_0} \\ 0 & \rho_0 c_0^2 & 0 \end{pmatrix}. \tag{8}$$

The matrices (A_1, A_2) are diagonalizable with eigenvalues $-c_0, 0, c_0$. The definition of a right absorbing layer concerns only the matrix A_1, and yields the SMART equation

$$\partial_t u + A_1 \partial_x u + A_2 \partial_z u + d(x)^+ B_1^+ u = s, \tag{9}$$

where B_1^+ is the projector on $Ker(A_1 - c_0 I)$ and $d(x)^+$ is a damping coefficient which is non-zero only in the right layer.

Properties of the SMART method

The main interesting property of the SMART method is its robustness. Provided the initial hyperbolic system is symmetrizable, the method is ensured to be dissipative: no amplification of the solution can be induced. Symmetrizable means that there exists a symmetric positive definite matrix S such that the matrices SA_i are symmetric. The proof of the dissipation property, based on energy estimates of the solution, is given in Métivier et al. (2014). The symmetrizability condition is satisfied by the general elasto-dynamic equations (Burridge, 1996).

The local decomposition of the wavefield provides a tool to distinguish between *P*-waves and *S*-waves. In the acoustic example above, only *P*-waves are simulated, and the matrices A_i have only 1 positive eigenvalue: the *P*-wave velocity. In more general 2D elasto-dynamic systems, the matrices A_i have two different positive eigenvalues v_P and v_S, corresponding to the *P*-waves and *S*-waves velocities. The definition of the projectors on the eigenspaces $ker(A_1 - v_P I)$ or $ker(A_1 - v_S I)$ yields the possibility of damping *P*-waves or *S*-waves. As shown in the numerical results, this yields a new method to prevent the generation of spurious *S*-waves in acoustic TI modeling. The damping of *S*-waves can be applied around the source in order to avoid directly their generation.

In terms of accuracy, the SMART method is not perfectly matched: the reflection coefficient at the interface between the domain of interest and the layer is not zero as soon as the incidence angle is different from zero. However, the SMART method only amounts to the introduction of a zero-order term in the initial equation. The computational cost of the SMART method is thus cheaper than conventional PML or CPML methods: for a fixed computational time, the SMART layer can be wider and may reach the accuracy of a PML.

NUMERICAL EXPERIMENTS

Acoustic TI equations

We consider the 2D acoustic TI equations proposed by Duve-

DOI http://dx.doi.org/10.1190/segam2014-0860.1

neck and Bakker (2011).

$$\begin{cases} \partial_t u_x = & \frac{1}{\rho}\partial_x\left(\cos^2\theta\sigma_{xx}+\sin^2\theta\sigma_{zz}\right)+ \\ & \frac{1}{\rho}\partial_z\left(\sin\theta\cos\theta\left(\sigma_{zz}-\sigma_{xx}\right)\right) \\ \partial_t u_z = & \frac{1}{\rho}\partial_z\left(\sin^2\theta\sigma_{xx}+\cos^2\theta\sigma_{zz}\right)+ \\ & \frac{1}{\rho}\partial_x\left(\sin\theta\cos\theta\left(\sigma_{zz}-\sigma_{xx}\right)\right) \\ \partial_t \sigma_{xx} = & \rho v_P^2\left(1+2\varepsilon\right) \\ & \left[\cos^2\theta\partial_x u_x-\sin\theta\cos\theta(\partial_x u_z+\partial_z u_x)+\sin^2\theta\partial_z u_z\right] \\ & +\rho v_P^2\sqrt{1+2\delta} \\ & \left[\sin^2\theta\partial_x u_x+\sin\theta\cos\theta(\partial_x u_z+\partial_z u_x)+\cos^2\theta\partial_z u_z\right] \\ \partial_t \sigma_{zz} = & \rho v_P^2\sqrt{1+2\delta} \\ & \left[\cos^2\theta\partial_x u_x-\sin\theta\cos\theta(\partial_x u_z+\partial_z u_x)+\sin^2\theta\partial_z u_z\right] \\ & +\rho v_P^2 \\ & \left[\sin^2\theta\partial_x u_x+\sin\theta\cos\theta(\partial_x u_z+\partial_z u_x)+\cos^2\theta\partial_z u_z\right]. \end{cases} \quad (10)$$

The system (10) is derived from the elasto-dynamic equations by setting the S-wave velocity to 0 in the stiffness tensor. In (10), v_P is the vertical P-wave velocity, ρ is the density. The anisotropy symmetry axis is defined by the tilt angle θ. The Thomsen anisotropy parameters are ε and δ. The velocity displacement in x and z directions are u_x, u_z, while σ_{zz} is the stress aligned with the symmetry axis of anisotropy and σ_{xx} is the stress tangential to this direction. We discretize these equations using a 4th order finite-difference scheme based on the rotated stencil proposed by Saenger and Bohlen (2004). The discretization in time is performed following a standard 2nd order leap-frog scheme.

BP 2007 model

We perform a comparison between the PML and SMART methods on a 2D model extracted from the BP 2007 TTI benchmark model. The model is presented in Figure 1. The density is taken constant equal to 1000 kg.m^{-3}.

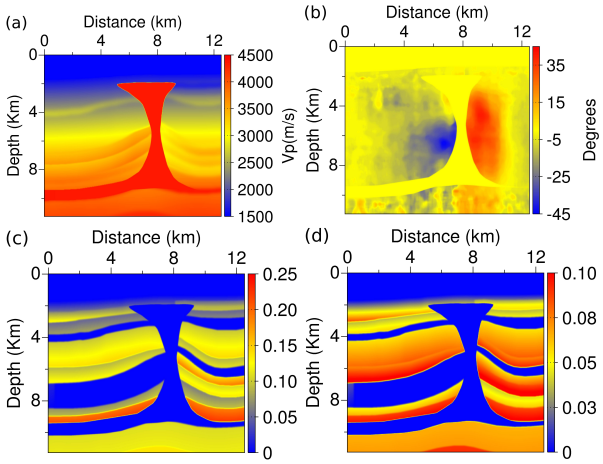

Figure 1: Model extracted from the BP 2007 benchmark model: (a) vertical P-wave velocity,(b) tilt angle, (c-d) Thomsen parameter ε and δ

Comparison between SMART and PML strategies

We consider a surface acquisition system. We use a Ricker explosive source located at $x_S = 6200$ m, $z_S = 50$ m. The Ricker signal is centered on 4 Hz. A free-surface condition is implemented on top. We use a spatial discretization step $h = 25$ m to ensure at least 5 grid points by minimal wavelength. The time discretization step is set to $\Delta t \simeq 2\times10^{-3}s$ according to the CFL condition. The total simulation time is $T = 12$ s. We compute a reference solution in a domain large enough to ensure no reflection at the external boundaries. The model is continuously extended in the direction normal to the interface. The reference seismogram and the residual seismograms corresponding to the PML and SMART methods are presented in Figure 2. The PML solution is computed with a 20 grid points width layer. Two SMART solutions are computed, with a respectively 20 and 30 grid points width layer. The seismograms

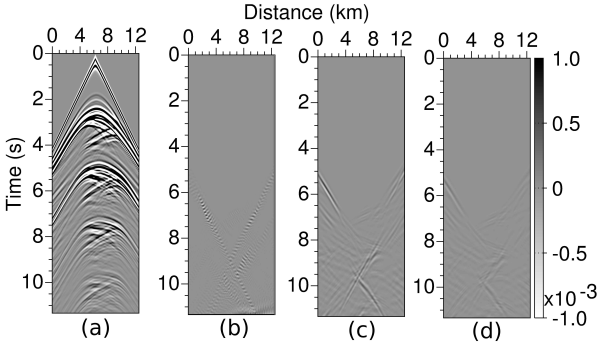

Figure 2: (a) Reference seismogram. (b) PML residuals with 20 grid points. (c) SMART residuals with 20 grid points and (d) 30 grid points.

give an insight of the accuracy of the methods. The color scale is purposely chosen to saturate the reference seismogram. The residuals seismograms show low energy associated to spurious reflections. The SMART method with 20 grid points width layer is less accurate than the PML in terms of these spurious reflections. Extending the layer to 30 grid points decreases their amplitude to the level of the ones generated by the PML.

In Figure 3, we present snapshots of the pressure wavefield computed at $t = 4.2$ s, 7.8 s and 12 s. The amplification yielded by the PML is clearly visible on row (b), starting at time $t = 7.8$ s on the right and bottom edges of the domain of interest. At final time $t = 12$ s, the spurious amplified wavefield contaminates almost all the domain of interest. Note that the amplified spurious wavefield does not reach the surface at final time, which explains why the amplification is not visible in the PML seismogram in Figure 2. Comparatively, the SMART layer method wavefield does not suffer from this amplification phenomenon (Fig. 3, row (c)).

A S-waves filter for acoustic TI modeling

Since the pioneering work of Alkhalifah (2000), acoustic TI equations have been derived to avoid the computational burden associated with the solution of TI elasto-dynamic equations. The acoustic approximation neglects the S-wave propagation while preserving the anisotropic effect on the propagation of P-waves. Following the strategy of Duveneck and Bakker (2011), the acoustic TI approximation consists in setting the S-wave velocity to 0 in the stiffness tensor (Duveneck and Bakker, 2011). However, in general TI media such that $\varepsilon > \delta$, this approximation results in a S-wave velocity which is 0 only along the symmetry axis and in the direction orthog-

DOI http://dx.doi.org/10.1190/segam2014-0860.1

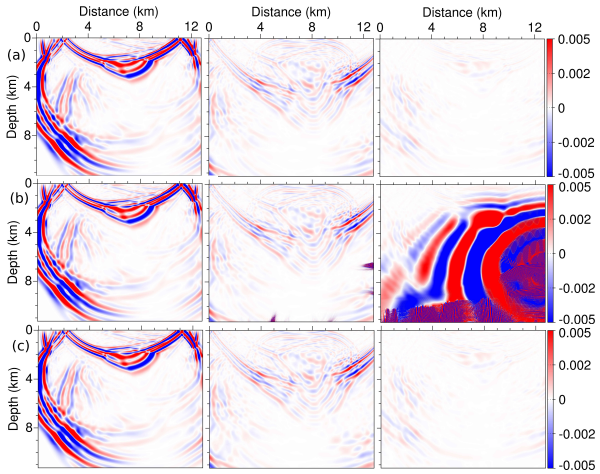

Figure 3: Pressure wavefield snapshots in the domain of interest at time $t = 4.2$ s, 7.8 s and 12 s. Reference wavefield (row a). PML wavefield (row b), SMART wavefield (row c). The PML amplification starts at time $t = 7.8$ s on the right and bottom edges of the domain and contaminates almost all the domain at final time $t = 12$ s.

onal to this axis. The *S*-wave velocity is non zero in arbitrary directions (Grechka et al., 2004). This causes the generation of non-physical *S*-waves. To mitigate this phenomenon, one possibility is to embed the source in a media such that $\varepsilon = \delta$ (elliptical anisotropy) (Duveneck et al., 2008), for which the *S*-wave velocity is zero in all directions. However, this requires to modify the subsurface model, and may also generate spurious reflections at the interface between the artificial zone and the true model. Another possibility is to weight the source explosion, as promoted by Operto et al. (2009). Although this reduces their amplitude, non-negligible *S*-waves remain.

We propose to complement the weighting strategy of Operto et al. (2009) with a SMART damping. We damp, around the source, the components of the wavefield propagating in x and z directions with a *S*-wave velocity. We first present results obtained in a homogeneous medium, such that $v_P = 2000$ m.s^{-1}, $\varepsilon = 0.3$, $\delta = 0.1$. A Ricker source centered on 15 Hz is used for this experiment. The simulation time is set to 2 s. In Figure 4, we compare snapshots of the wavefield obtained in a reference domain (using only the source weighting strategy proposed by Operto et al. (2009)) with snapshots of the wavefield obtained combining weighting and *S*-wave damping at the source. The amplitude scale is chosen to emphasize the presence of spurious *S*-waves around the source. The SMART damping allows us to efficiently decrease the amplitude of the *S*-waves.

We complement this analysis with the comparison of seismograms in the BP 2007 model. In the experiments presented in Figures 2 and 3, no *S*-waves are generated, as the source is located in the water at the top of the model: the *S*-wave velocity is 0 in all directions around the source. We thus relocate the source at $x_S = 10.5$ km, $z_S = 2$ km, in a TI zone of the model. We compute a reference seismogram in a domain large enough to ensure no reflection at the external boundaries. We compare

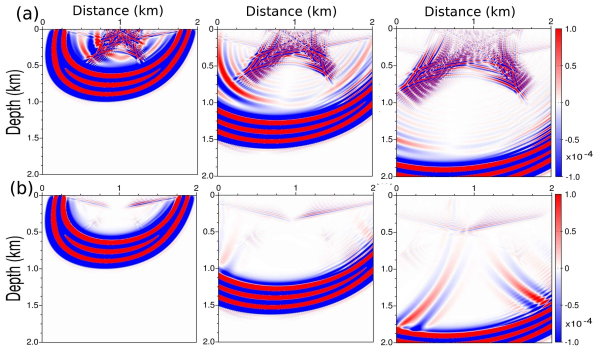

Figure 4: Pressure wavefield snapshots in the domain of interest at time $t = 0.45$ s, $t = 0.75$ s, $t = 1.15$ s. Reference wavefield (row a). SMART wavefield with *S*-wave filter (row b). The *S*-waves damping allows to efficiently filter spurious *S*-waves at the source.

it with the SMART seismograms obtained with a damping of the *S*-waves around the source (Fig. 5). The imprint of the *S*-waves is strongly damped in the SMART seismograms.

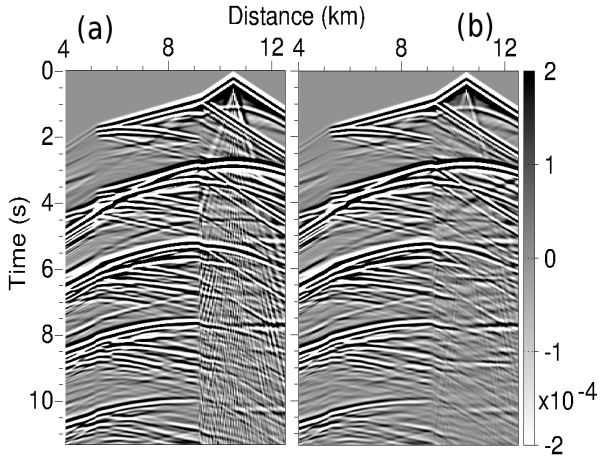

Figure 5: Seismograms in the BP 2007 model with a source located at $x_S = 10.5$ km, $z_S = 2$ km. The imprint of *S* waves, clearly visible in the reference seismogram (a), is efficiently decreased in the SMART seismogram (b).

CONCLUSION

The SMART layer method is an appropriate alternative to the PML method for seismic wave simulation in anisotropic media. For these media, the PML becomes amplifying, while the SMART layer ensures the dissipation of the energy. For acoustic TI modeling, the SMART method formulation also gives the possibility to damp directly at the source the spurious *S*-waves. The accuracy provided by a standard PML can be reached at the expense of an increase of the SMART layer size. This increase is compensated by the fact that the SMART method is less expensive in terms of computational cost as it only amounts to adding a zero-order term to the initial equations. Further experiments will be performed to assess the interest of the method for imaging algorithms such as FWI and RTM.

DOI http://dx.doi.org/10.1190/segam2014-0860.1

http://dx.doi.org/10.1190/segam2014-0860.1

EDITED REFERENCES

Note: This reference list is a copy-edited version of the reference list submitted by the author. Reference lists for the 2014 SEG Technical Program Expanded Abstracts have been copy edited so that references provided with the online metadata for each paper will achieve a high degree of linking to cited sources that appear on the Web.

REFERENCES

Alkhalifah, T., 2000, An acoustic wave equation for anisotropic media: Geophysics, **65**, 1239–1250, http://dx.doi.org/10.1190/1.1444815.

Bécache, E., S. Fauqueux, and P. Joly, 2003, Stability of perfectly matched layers, group velocities and anisotropic waves: Journal of Computational Physics, **188**, no. 2, 399–433, http://dx.doi.org/10.1016/S0021-9991(03)00184-0.

Bérenger, J.-P., 1994, A perfectly matched layer for absorption of electromagnetic waves: Journal of Computational Physics, **114**, no. 2, 185–200, http://dx.doi.org/10.1006/jcph.1994.1159.

Burridge, R., 1996, Elastic waves in anisotropic media: Schlumberger-Doll Research internal report, accessed 9 June 2014, math.stanford.edu/pub/mgss/burridge2.ps.gz.

Cerjan, C., D. Kosloff, R. Kosloff, and M. Reshef, 1985, A nonreflecting boundary condition for discrete acoustic and elastic wave equations: Geophysics, **50**, 705–708, http://dx.doi.org/10.1190/1.1441945.

Duveneck, E., and P. M. Bakker, 2011, Stable P-wave modeling for reverse-time migration in tilted TI media: Geophysics, **76**, no. 2, S65–S75, http://dx.doi.org/10.1190/1.3533964.

Duveneck, E., P. Milcik, P. M. Bakker, and C. Perkins, 2008, Acoustic VTI wave equations and their application for anisotropic reverse-time migration: 78th Annual International Meeting, SEG, Expanded Abstracts, 2186–2190.

Engquist, B., and A. Majda, 1977, Absorbing boundary conditions for numerical simulation of waves: Mathematics of Computation, **31**, no. 139, 629–651.

Grechka, V., L. Zhang, and J. W. Rector III, 2004, Shear waves in acoustic anisotropic media: Geophysics, **69**, 576–582, http://dx.doi.org/10.1190/1.1707077.

Halpern, L., S. Petit-Bergez, and J. Rauch, 2011, The analysis of matched layers: Confluentes Mathematici, **3**, no. 2, 159–236, http://dx.doi.org/10.1142/S1793744211000291.

Israeli, M., and S. A. Orszag, 1981, Approximation of radiation boundary conditions: Journal of Computational Physics, **41**, no. 1, 115–135, http://dx.doi.org/10.1016/0021-9991(81)90082-6.

Komatitsch, D., and R. Martin, 2007, An unsplit convolutional perfectly matched layer improved at grazing incidence for the seismic wave equation: Geophysics, **72**, no. 5, SM155–SM167, http://dx.doi.org/10.1190/1.2757586.

Operto, S., J. Virieux, A. Ribodetti, and J. E. Anderson, 2009, Finite-difference frequency-domain modeling of viscoacoustic wave propagation in 2D tilted transversely isotropic (TTI) media: Geophysics, **74**, no. 5, T75–T95, http://dx.doi.org/10.1190/1.3157243.

Saenger, E. H., and T. Bohlen, 2004, Finite-difference modeling of viscoelastic and anisotropic wave propagation using the rotated staggered grid: Geophysics, **69**, 583–591, http://dx.doi.org/10.1190/1.1707078.